

Clonal expansion of CAR-T cells harboring lentivector integration in the PLAAT4 gene following anti-CD19 CAR T-cell therapy in a context of cutaneous T-cell lymphoma

by Vincent Guiraud, Clotilde Bravetti, Amélie Guihot, Jérôme Alexandre Denis, Ronan Legrand, Frédéric Charlotte, Magali Le Garff-Tavernier, Christophe Parizot, Baptiste Fouquet, Roch Houot, Remy Dulery, Anne-Genevieve Marcelin, Vincent Calvez, Stéphane Barete, Eve Todesco and Sylvain Choquet

Received: March 9, 2026.

Accepted: June 3, 2026.

Citation: Vincent Guiraud, Clotilde Bravetti, Amélie Guihot, Jérôme Alexandre Denis, Ronan Legrand, Frédéric Charlotte, Magali Le Garff-Tavernier, Christophe Parizot, Baptiste Fouquet, Roch Houot, Remy Dulery, Anne-Genevieve Marcelin, Vincent Calvez, Stéphane Barete, Eve Todesco and Sylvain Choquet. Clonal expansion of CAR-T cells harboring lentivector integration in the PLAAT4 gene following anti-CD19 CAR T-cell therapy in a context of cutaneous T-cell lymphoma.

Haematologica. 2026 June 11. doi: 10.3324/haematol.2026.300851 [Epub ahead of print]

Publisher's Disclaimer.

E-publishing ahead of print is increasingly important for the rapid dissemination of science.

Haematologica is, therefore, E-publishing PDF files of an early version of manuscripts that have completed a regular peer review and have been accepted for publication.

E-publishing of this PDF file has been approved by the authors.

After having E-published Ahead of Print, manuscripts will then undergo technical and English editing, typesetting, proof correction and be presented for the authors' final approval, the final version of the manuscript will then appear in a regular issue of the journal.

All legal disclaimers that apply to the journal also pertain to this production process.

Clonal expansion of CAR-T cells harboring lentivector integration in the PLAAT4 gene following anti-CD19 CAR T-cell therapy in a context of cutaneous T-cell lymphoma

Vincent Guiraud ¹, Clotilde Bravetti ², Amélie Guihot ³, Jérôme Alexandre Denis ⁴, Ronan Legrand ⁴, Frédéric Charlotte ⁵, Magali Le Garff-Tavernier ², Christophe Parizot ³, Baptiste Fouquet ³, Roch Houot ⁶, Remy Dulery ^{7,8}, Anne-Genevieve Marcelin ¹, Vincent Calvez ¹, Stéphane Barete ⁹, Eve Todesco ¹, Sylvain Choquet ¹⁰

¹ Sorbonne University, INSERM, Institut Pierre Louis d'Epidémiologie et de Santé Publique (IPLESP), Assistance Publique-Hôpitaux de Paris (AP-HP), Pitié-Salpêtrière Hospital, Virology department, Paris, France; ²Sorbonne University, Paris, France, Department of Biological Hematology, Pitié-Salpêtrière Hospital, Assistance Publique-Hôpitaux de Paris, Paris, France; ³Sorbonne Université, INSERM U1135, Center for Immunology and Infectious Diseases (CIMI), Department of Immunology, Assistance Publique-Hôpitaux de Paris, Pitié-Salpêtrière Hospital, Paris, France; ⁴Sorbonne University, INSERM UMRS-938, Saint-Antoine Research Center, TGF- β , signalisation cellulaire et cancer, Department of Endocrine and Oncological Biochemistry, Unit of Cellular and Molecular Oncobiology, AP-HP, Pitié-Salpêtrière Hospital, Assistance Publique – Hôpitaux de Paris, Paris, France; ⁵Sorbonne University, Department of Pathological Anatomy and Cytology, Assistance Publique-Hôpitaux de Paris, Hôpital Pitié-Salpêtrière Charles Foix, Paris, France; ⁶Department of Hematology, University Hospital of Rennes, UMR U1236, INSERM, University of Rennes, French Blood Establishment, Rennes, France; ⁷Sorbonne University, Department of Clinical Hematology and Cellular Therapy, Hôpital Saint-Antoine, Assistance Publique—Hôpitaux de Paris, INSERM, UMRs 938, Centre de recherche Saint-Antoine (CRSA), Paris, France; ⁸Department of Medical Oncology, Dana-Farber Cancer Institute, Harvard Medical School, Boston, USA; ⁹Sorbonne University, Unit of Dermatology, Pitié-Salpêtrière Hospital, Assistance Publique – Hôpitaux de Paris, Paris, France and ¹⁰Sorbonne University, Department of Clinical Hematology, Pitié-Salpêtrière Hospital, Assistance Publique – Hôpitaux de Paris, Paris, France

Correspondence:

Vincent Guiraud, M.D., PhD
83 Bd de l'Hôpital, 75013 Paris, France
Tel: +33 1 42 17 74 01 / Fax: +33 1 42 17 74 11
Email: vincent.guiraud@aphp.fr

Declaration of competing interests: The authors declare no conflict of interest in relation with this study.

Fundings: This work was supported in part by the ANRS-MIE (Agence Nationale de Recherches sur le SIDA et les hépatites virales-Maladies Infectieuses Emergentes - Medical and Pharmacological ANRS-MIE Network) and the Groupe Pasteur Mutualité. Study sponsors had no part on study design, data

collection, data analyses, data interpretation, manuscript writing nor decision to submit for publication.

Running Title: Clonal CAR proliferation in a cutaneous T-lymphoma

Keywords: T-cell lymphoma, Chimeric antigen receptor T-cell, PLAAT4, clonal proliferation, second primary malignancy

Data availability statement

The data that support the findings of this study are available from the corresponding author upon reasonable request.

Author contributions

VG, VC, SB, ET, SC: data curation, conceptualization, methodology, formal analysis, writing - original draft. CB, AG, JAD, RL, FC, MLG, CP, AGM: data curation, formal analysis, writing - review and editing.

RD, RH: writing - review and editing.

Chimeric antigen receptor (CAR) T-cell therapies have emerged as groundbreaking treatments for high-grade hematological malignancies, extending progression-free and overall survival ¹. However, because CAR-T cell production relies on viral vectors that integrate into host cell DNA, this raises a specific safety concern that CAR integration might disrupt gene expression associated with cell proliferation, ultimately contributing to T-cell malignancies ². Two mechanisms have been associated with retroviral-induced malignancies: either vector insertion leading to the inactivation of a tumor suppressor gene ³, or activation of nearby proto-oncogenes through its transcriptional enhancers ⁴.

We recently reported, in a large cohort study, a case of T-cell lymphoma in which a minor CAR T-cell population, dominated by a CAR clone integrated into the *PLAAT4* (*Phospholipase A and Acyltransferase 4*) gene, expanded ⁵. This work details the characteristics of this clone and its evolution during the course of the T-cell lymphoma.

We performed the following evaluations. First, we retrospectively evaluated clinical outcomes of all patients with a history of tisagenlecleucel (tisa-cel) treatment at Pitié-Salpêtrière Hospital (Paris, France). We extracted all consecutive blood CAR-T cell levels from the medical records of the complete-responders subpopulation, as their levels have been correlated with vector and clinical response ^{6,7}, to determine whether CAR-T cells blood levels could have warned us about the incident T-cell lymphoma. Then, integration site analyses were performed using a modified Integration Site Loop Amplification (ISLA) ^{8,9} to determine the exact locations of CAR transgene integration sites. Clone quantifications were performed using integration-specific primers for each CAR-T cell clone, along with a lentiviral-specific primer (1.U5) and a unique probe targeting the 3' end of the lentiviral transgene. Primer specificity was assessed using the patient's pre-CAR-T cell genomic DNA. Quantification was performed in duplicate and normalized to the RPP30 gene on a Qx200 digital droplet PCR platform (Bio-Rad, Hercules, USA). T-cell receptor gamma (TCR γ) clonality was assessed as reported ¹⁰ on an Illumina™ MiSeq platform. Clonotype assignment was performed using Vidjil ¹¹. TRGV/TRGJ annotation and CDR3 characterization were performed using IMGT V-QUEST ¹². Sixty-one relevant genes were sequenced on an Illumina™ MiSeq platform from fresh skin biopsy samples using the Sure Select panel (Agilent, Santa Clara, California): *ARID1A*, *ATM*, *B2M*, *BCL2*, *BCOR*, *BIRC3* (exons 7 to 10), *BRAF* (exon15), *BTK*, *CARD11* (exons 4 to 10), *CCL22* (exons 2 and 3), *CCND3* (exon 5), *CCND1* (exon 1), *CD28*, *CD37*, *CD79A* (exons 4 and 5), *CD79B*, *CREBBP*, *CXCR4*, *DNMT3A*, *EGR2*, *EP300*, *EZH2* (exons 16 to 17), *FBXW7*, *ID3*, *GNA13*, *IDH2* (exon 4), *IGLL5*, *JAK1* (exons 14 to 25), *JAK3*, *KLF2*, *KMT2D*, *KRAS*, *MYC*, *MYD88* (exons 3 to 5), *NFKBIE*, *NOTCH1* (exon 34 to 3'UTR), *NOTCH2* (exon 34 and 3'UTR), *PIM1*, *PLCG1*, *PLCG2*, *POT1*, *PRDM1* (exons 1 and 2), *PTPN1* (exons 2 to 6), *PTPRD*, *RHOA*, *RPS15*, *SAMHD1*, *SF3B1* (exons 12 to 18), *SMARCA4*, *SPI1* (exon 5), *STAT3* (exons 19 to 21), *STAT5B* (exons 14 to 17), *STAT6* (exon 12 to 18), *TBL1XR1*, *TCF3*, *TET2*, *TNFAIP3*, *TNFRSF14* (exons 2 and 4), *TP53*, *XPO1* (exon 15). Variant detection threshold was set at 2%. *CREBBP* exon31 was amplified using reported primer sets ¹³ and Sanger sequenced with the same primers. Statistical analyses and figures were performed using R or GraphPad Prism v9.0. This study was conducted in accordance with the Declaration of Helsinki, and written informed consent was obtained from the patient.

A 70-year-old woman received tisa-cel as fourth-line therapy for a stage IV Ann Arbor diffuse large B-cell lymphoma with central nervous system involvement. Complete remission was achieved one month post infusion.

As reported ⁵, T-cell lymphoma occurred 18 months after infusion, initially presenting as a skin nodule on the left shoulder which prompted an outpatient skin biopsy revealing a dense dermal infiltrate of small T-lymphocytes. Three years post-infusion, following a community-acquired pneumonia and a femoral neck fracture, the patient was definitively diagnosed with cutaneous CD30+ T-cell non-Hodgkin lymphoma (NHL) in the setting of numerous hypermetabolic centimetric skin nodules, without

argument for lymph node involvement (figure 1). At this time, her CAR-T cells levels in blood were comparable to the other tisa-cel complete responders (supplementary figure 1). Biopsy was remarkable for atypical CD3+, CD30+, CD20-, CD4-, CD8-, CD2-, CD5-, CD7-, CD25-, Granzyme B-, ALK1-, MUM1+ cells, with a Ki-67 proliferation index of 80%. TCR- γ sequencing identified two predominant productive clonal rearrangements in the biopsy: TRGV10-JP1 and TRGV3-JP2 accounting for 58% and 20% of the analyzed sequences, respectively (supplementary figure 2). The two lymphoma clones were also found in blood, representing 2% and 0.4% of the reads, respectively. Importantly, T-cell clonality showed a polyclonal pattern before CAR-T cell infusion, without detection of the two lymphoma clones nor the main CAR-T cell clone (supplementary figure 3). Targeted sequencing of the biopsy uncovered an undescribed missense mutation in exon 31 of the CREBBP tumor suppressor gene (c.5381C>T, p.(Ser1794Phe)), with a variant allele fraction of 37%.

The patient was treated with photochemotherapy for the T-cell lymphoma, with no clinical response, followed by brentuximab-vedotin, which resulted in a partial response after 3 cycles. Upon relapse, low-dose gemcitabine (75 mg/m², D1-D15) was initiated due to grade 3 neutropenia and grade 2 thrombopenia. Clinical course was further complicated by bronchiolitis, a second femoral neck fracture, recurrent falls, and the patient died of septic shock due to a urinary tract infection four years post CAR-T cell infusion, in complete response for the T-cell NHL.

Due to the T-cell nature of the lymphoma, blood and biopsy samples were simultaneously analyzed for CAR-T cell quantification. At 3 years post-infusion, CAR-T cells were 28-fold more enriched in the skin biopsy than in peripheral blood (5.1% vs 0.18% of total cells).

As reported ⁵, *PLAAT4* was the predominant site of CAR transgene integration in the biopsy. Further investigation retrieved additional sites, including *SETX*, *MEIOB*, and *ZNF512*. Among all CAR-positive clones, *PLAAT4* remained the most frequent, representing 54.1% of all CAR integration events, while *SETX*, *MEIOB*, and *ZNF512* accounted for 23.0%, 10.8%, and 6.8%, respectively. In a second cutaneous biopsy collected during disease relapse after treatment with brentuximab vedotin, the frequency of the *PLAAT4* clone increased to 80% of all CAR-T cells. Notably, none of the three minor clones identified in the initial biopsy were detected using the same assay (figure 2).

Integration site analyses were performed on whole blood samples collected at peak expansion post-infusion (day 15 post-infusion) and at the time of T-cell lymphoma diagnosis (three years post-infusion). At peak expansion, the CAR-T cell population was polyclonal, without detection of the *PLAAT4* clone. At the time of lymphoma diagnosis, the *PLAAT4* clone was predominant, accounting for 60% of all CAR-T cells, alongside six minor clones, each comprising less than 5% of the total CAR-T cell population (figure 2).

To investigate the longitudinal dynamics of CAR-T cell clones, peripheral blood samples collected at 18 time points following CAR-T cell infusion were analyzed using integration-specific digital droplet PCR (figure 3). The *PLAAT4* clone became detectable around 200 days post-infusion, followed by a rapid eightfold expansion approximately three years post-infusion, coinciding with the diagnosis of T-cell malignancy. A transient decrease was measured during brentuximab vedotin treatment, associated with a transient clinical response. A second expansion peak emerged during disease relapse under brentuximab vedotin treatment. Apart from the dominant clone, no clone consistently represented >5% of the total CAR-T cell pool. The *MEIOB* and *SETX* CAR clones were never detected in blood.

CAR-T cells were sorted from a blood sample collected at the time of disease relapse. None of the major lymphoma-associated TCR γ clonal rearrangements were detected in the sorted CAR-T cell population (supplementary figure 4). In addition, the CREBBP missense mutation identified in the lymphoma biopsy was not detected in these cells.

Finally, to assess lymphocyte survival, during the T-cell lymphoma relapse, the patient's peripheral blood mononuclear cells (PBMCs) were isolated from whole blood and plated in RPMI-1640 glutamax (Gibco) supplemented with 10% fetal bovine serum to evaluate lymphocyte survival. Lymphocyte mortality was expected to reach 90% at one month and >99% at two months. CAR-T cells persisted for two months, accounting for 2–4% of total cells. The *PLAAT4* clone rose from two-thirds to 100% of the CAR-T cell population between one and two months of culture, suggesting a survival advantage, though no cell expansion was observed and we were unable to demonstrate that this clone was immortalized.

We report a case of T-cell lymphoma associated with a minor CAR-T cell population. While transformation of CAR-T cells into a tumor was unlikely, integration of the CAR transgene into the *PLAAT4* gene might have represented a genetic event contributing to the development or progression of the T-cell malignancy, as supported by the longitudinal analysis of clonal CAR populations.

This case contrasts with previous reports of CAR-T cells involvement in lymphomas. To date, all T-cell lymphomas occurring after CAR-T cell infusions have presented rather unequivocal findings: they were either monoclonal or oligoclonal CAR-T cell lymphomas, or CAR-T cells were absent from the biopsy samples¹⁴. In contrast, this lymphoma is characterized by the uncommon presence of two major non-CAR clones alongside a minor CAR-T cell population dominated by the *PLAAT4* clone.

We hypothesized that integration into the *PLAAT4* tumor suppressor gene might have contributed to the lymphoma, as this gene is frequently dysregulated in malignancies⁵. This longitudinal analysis, notably the delayed emergence and subsequent selection of the *PLAAT4* clone, also argues in favor of its potential involvement, as expansion of a major clonal CAR-T cell population is a highly uncommon event, reported in fewer than 2200 patient-years of follow-up¹⁵. In contrast, mono- or oligoclonal CAR-T cell populations have been consistently linked to malignancies¹⁴, except for the *TET2* clonal expansion case¹⁶. However, despite our comprehensive analysis of this case, we provide only indirect but convergent arguments regarding a potential link between the *PLAAT4* clone and the second primary malignancy. Also, few reports have emphasized that the integration site is only one of multiple contributing factors, and that CAR-T cell populations can undergo successive waves of expansion, driven primarily by T cell phenotype¹⁷ or, in some cases, by their integration sites¹⁸. Consequently, we still cannot formally exclude the possibility that a non-malignant CAR clonal population evolved alongside the two lymphoma clones.

Despite this rare event, our findings do not challenge the overall favorable safety profile of lentiviral CAR-T cell therapies. Rather, they highlight the importance of long-term molecular monitoring to better understand the biological determinants of CAR-T cell persistence and clonal dynamics.

References

1. Larson RC, Maus MV. Recent advances and discoveries in the mechanisms and functions of CAR T cells. *Nat Rev Cancer*. 2021;21(3):145-161.
2. Nienhuis AW, Dunbar CE, Sorrentino BP. Genotoxicity of retroviral integration in hematopoietic cells. *Mol Ther*. 2006;13(6):1031-1049.
3. Perica K, Jain N, Scordo M, et al. CD4+ T-cell lymphoma harboring a chimeric antigen receptor integration in *TP53*. *N Engl J Med*. 2025;392(6):577-583.
4. Hacein-Bey-Abina S, Von Kalle C, Schmidt M, et al. *LMO2* -associated clonal T cell proliferation in two patients after gene therapy for SCID-X1. *Science*. 2003;302(5644):415-419.
5. Dulery R, Guiraud V, Choquet S, et al. T cell malignancies after CAR T cell therapy in the DESCAR-T registry. *Nat Med*. 2025;31(4):1130-1133.
6. Wittibschlager V, Bacher U, Seipel K, et al. CAR T-cell persistence correlates with improved outcome in patients with b-cell lymphoma. *Int J Mol Sci*. 2023;24(6):5688.
7. Hanajiri R, Wakabayashi H, Ishigiwa K, et al. Robust CAR T-cell expansion and superior outcomes in DLBCL patients in complete response at infusion. *Br J Haematol*. 2025;207(1):180-188.
8. Guiraud V, Denis JA, Benhafoun G, et al. Longitudinal analysis of lentiviral and retroviral chimeric antigen receptors' integration sites reveals distinct clonal evolutionary patterns. *Br J Haematol*. 2025;206(4):1173-1177.
9. Guiraud V, Denis JA, Ben Attia S, et al. Development of a new high-yield integration site assay reveals disease-specific patterns across HTLV-1-associated pathologies. *Microbiol Spectr*. 2025;13(5):e0320824.
10. Armand M, Derrieux C, Beldjord K, et al. A new and simple TRG multiplex PCR assay for assessment of t-cell clonality: a comparative study from the EuroClonality Consortium. *Hemasphere*. 2019;3(3):e255.
11. Duez M, Giraud M, Herbert R, Rocher T, Salson M, Thonier F. Vidjil: a web platform for analysis of high-throughput repertoire sequencing. *PLoS One*. 2016;11(11):e0166126.
12. Manso T, Folch G, Giudicelli V, et al. IMGT® databases, related tools and web resources through three main axes of research and development. *Nucleic Acids Res*. 2022;50(D1):D1262-D1272.
13. Coupry I. Molecular analysis of the CBP gene in 60 patients with Rubinstein-Taybi syndrome. *J Med Genet*. 2002;39(6):415-421.
14. Maurer K, Jacobson CA. T-cell neoplasias and secondary malignancies after CAR-T cell therapy: current knowledge, risk factors, and implications from CAR-T engineering strategies. *Leuk Lymphoma*. 2025;66(7):1189-1197.
15. Jadowsky JK, Hexner EO, Marshall A, et al. Long-term safety of lentiviral or gammaretroviral gene-modified T cell therapies. *Nat Med*. 2025;31(4):1134-1144.
16. Fraietta JA, Nobles CL, Sammons MA, et al. Disruption of TET2 promotes the therapeutic efficacy of CD19-targeted T cells. *Nature*. 2018;558(7709):307-312.

17. Melenhorst JJ, Chen GM, Wang M, et al. Decade-long leukaemia remissions with persistence of CD4+ CAR T cells. *Nature*. 2022;602(7897):503-509.
18. Shah NN, Qin H, Yates B, et al. Clonal expansion of CAR T cells harboring lentivector integration in the CBL gene following anti-CD22 CAR T-cell therapy. *Blood Adv*. 2019;3(15):2317-2322.

Figure 1: Clinical lesions.

(A) Skin lesion of the left arm, (B) Nodular skin T-cell lymphoma on the neck, (C) Cutaneous hypermetabolism associated with T-cell lymphoma on CT-PET.

Figure 2: Clonality Based on Integration Site Analysis

CAR-T transgene integration sites from biopsy samples collected at (A) T-cell lymphoma diagnosis and (B) relapse of primary cutaneous CD30+ T-cell lymphoproliferative disorder, and in blood samples at 15 days post CAR-T cell infusion (C) and at time of the T-cell lymphoma diagnosis (D). Analyses were performed using the Integration Site Loop Amplification (ISLA) assay. Clones are labeled according to their host genes.

Figure 3: Longitudinal Evolution of the Total CAR Population and CAR clones in Blood Post-CAR T Infusion using ddPCR

The pink line represents the total CAR-T cell population, while the other lines represent each clonal population. The *PLAAT4* clone was not detected in blood before 200 days post-infusion. Arrows mark the time of T cell malignancy diagnosis, initiation of brentuximab vedotin treatment and disease relapse. Quantification was normalized to the housekeeping gene RPP30.

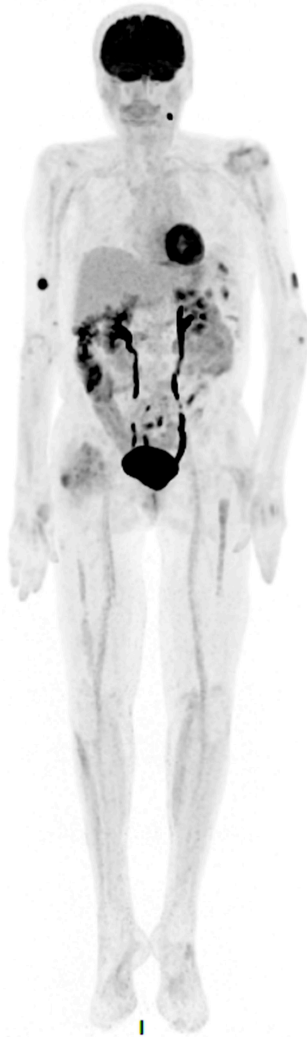
A



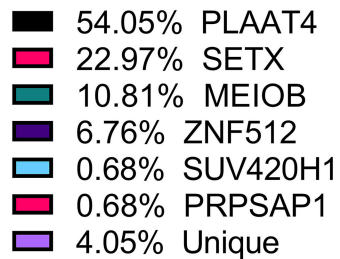
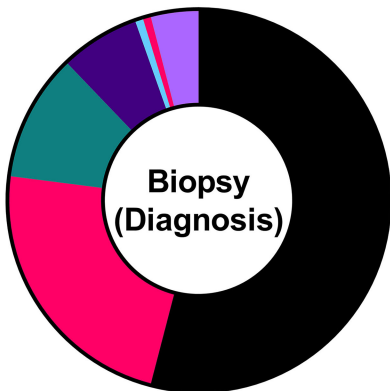
B



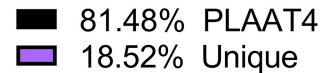
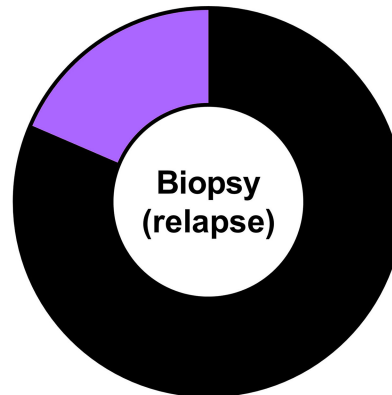
C



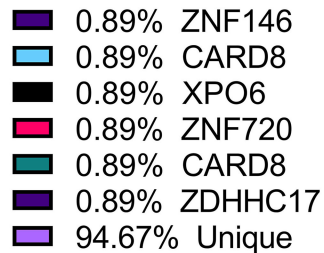
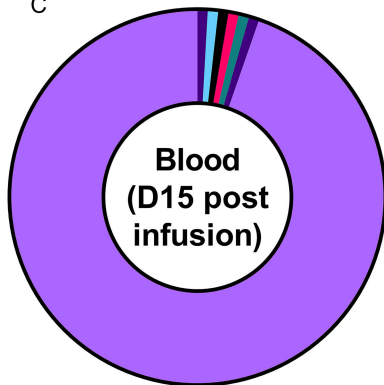
A



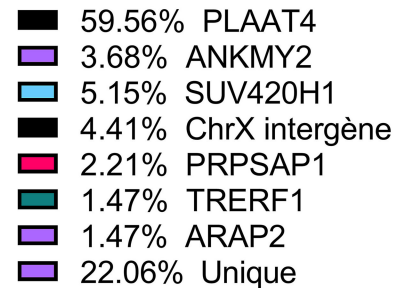
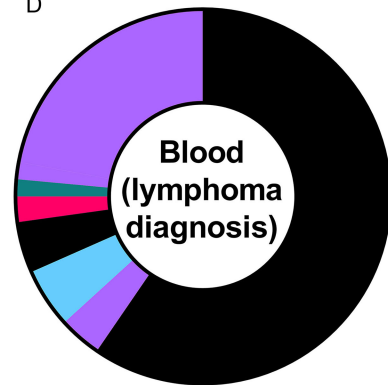
B

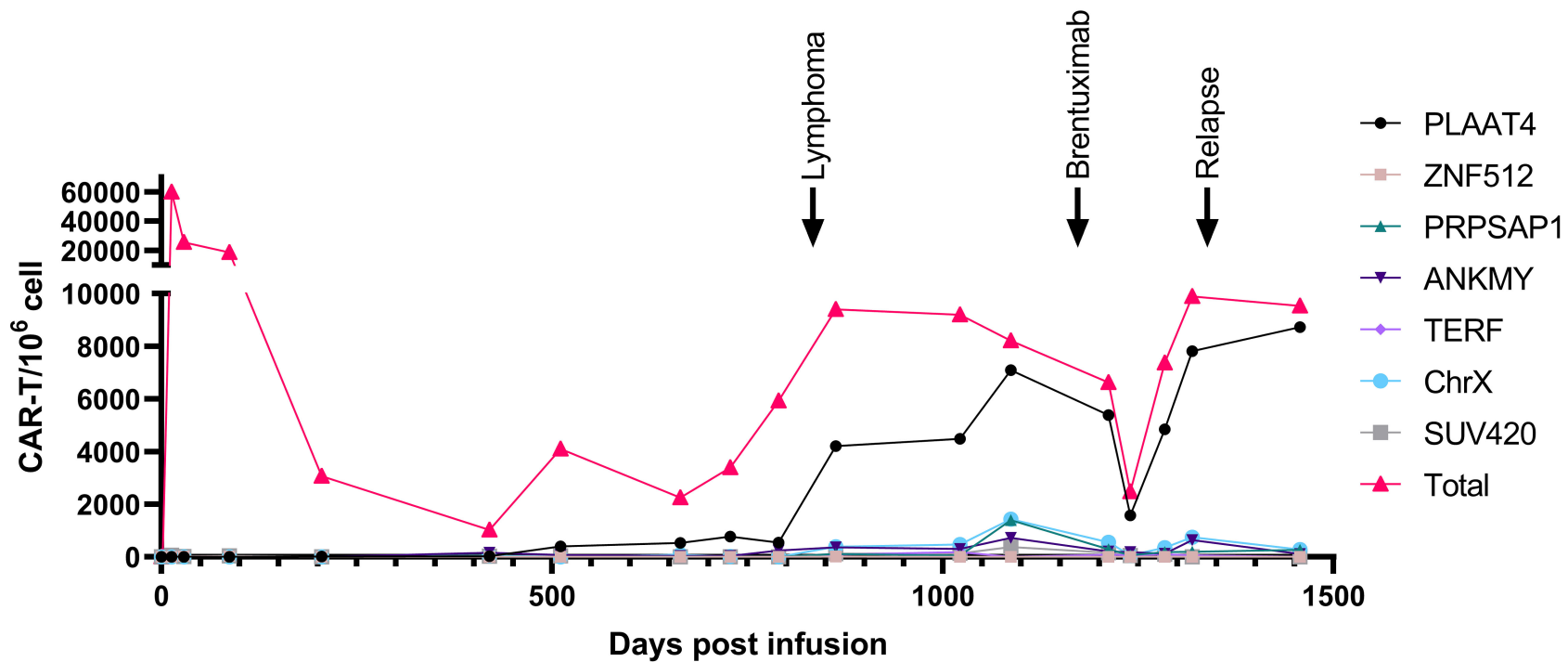


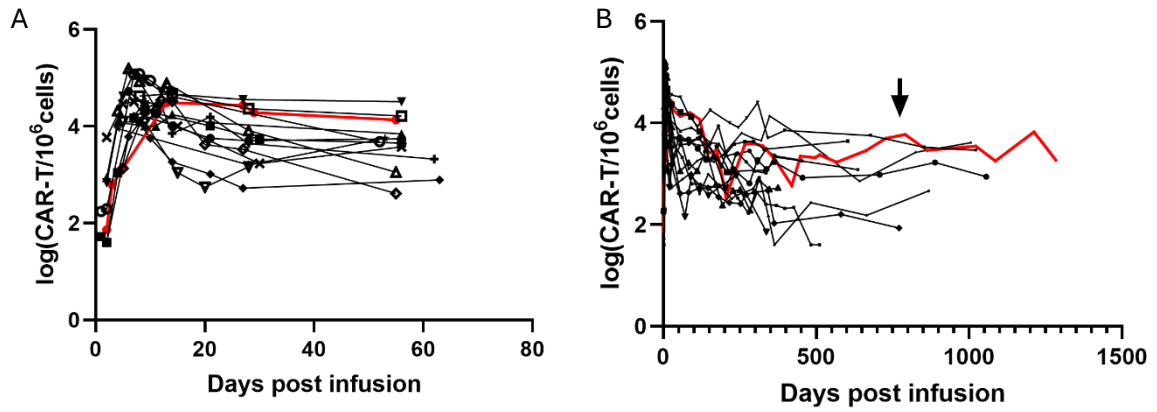
C



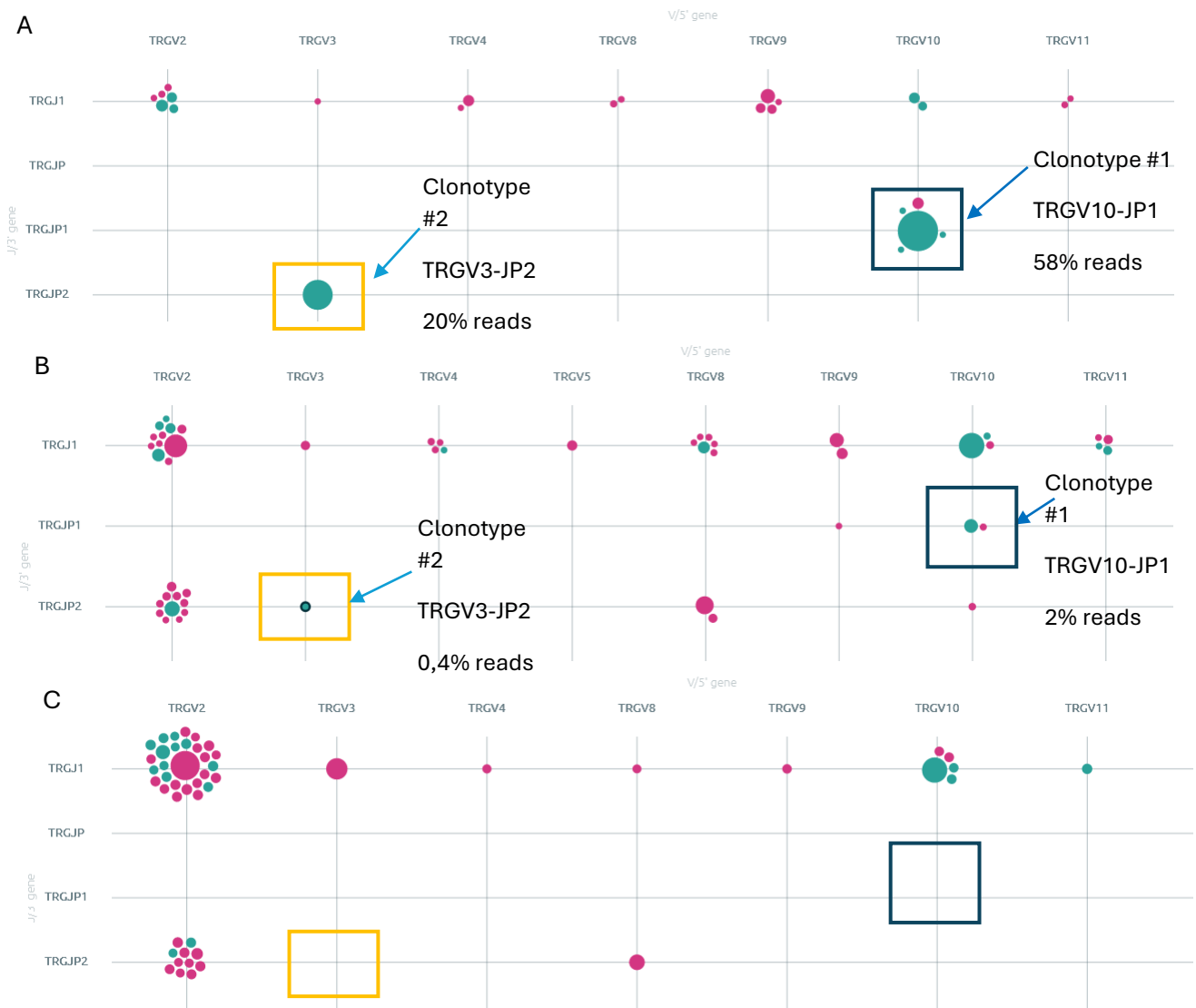
D



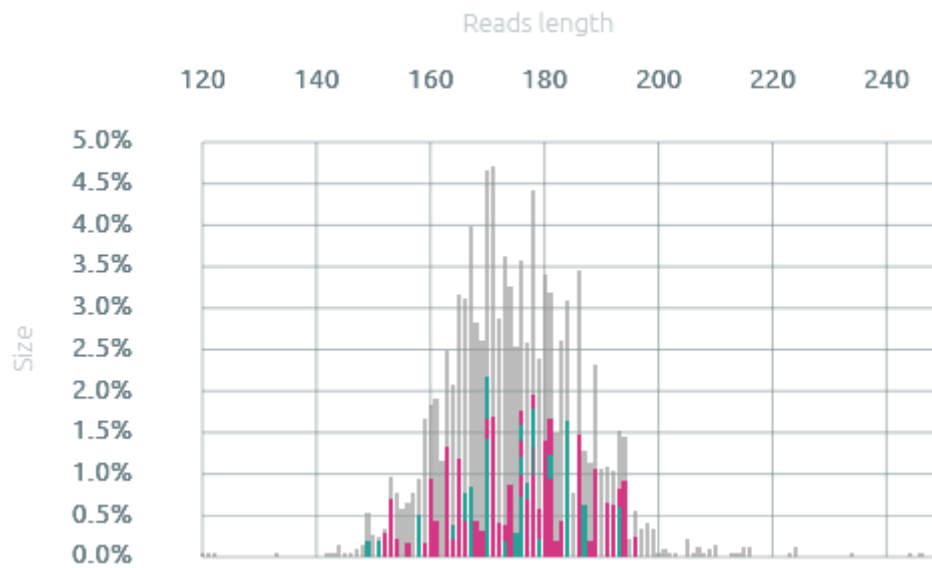




Supplementary figure 1: Blood CAR-T cell peak expansion (A) and plateau phase (B) for the patient with T-lymphoma (red line) compared to all other complete-responders patients treated with tisa-cel (black lines) at our center (n=14). Arrow represents T-cell lymphoma occurrence.

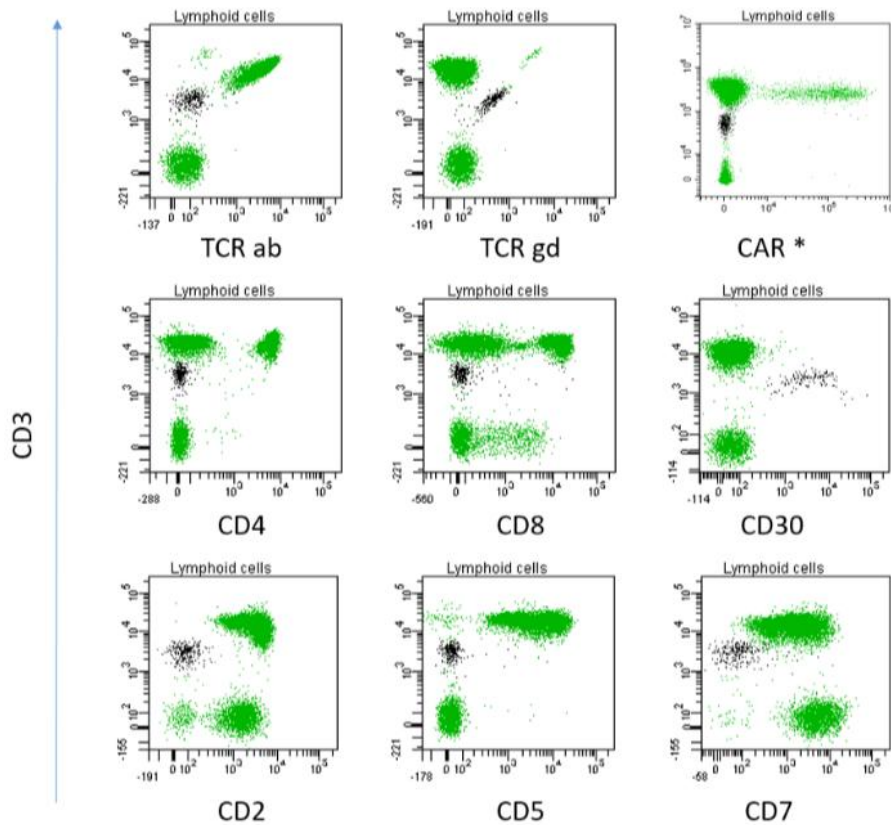


Supplementary figure 2: Vidjil-grid display of TCRgamma sequences obtained from NGS analysis. Clonotypic TRGV/TRGJ gene rearrangements are represented as bubbles sized according to their frequency. Green bubbles indicate productive rearrangements, pink bubbles the unproductive ones. A: T-cell pre-treatment lymphoma skin biopsy: two dominant productive clonal rearrangements are observed. One (TRGV10-JP1) represents 58% of reads. The other (TRGV3-JP2) represents 20% of the read. B: Peripheral blood at time of lymphoma diagnosis. The same two clonal rearrangements were found but at very low proportion (2% and 0.4% of reads respectively). C: Peripheral blood CAR cells sorting during relapse: none of the major tumor clonal rearrangement was detectable.



Supplementary figure 3 Vidjil-graphic display of TCRgamma sequences obtained in blood from NGS analysis before the CAR-T cell infusion

Clonotypic TRGV/TRGJ gene rearrangements are represented as bars. The x-axis shows the size of the rearrangement and the y-axis shows the frequency of the rearrangement. Green bars indicate productive rearrangements, pink bars the unproductive ones. In the blood collected less than a year before the CAR-T cell infusion, the profile is polyclonal and neither of the two rearrangements identified in the biopsy (TRGV10-JP1 and TRGV3-JP2) are detected, even at low frequency.



Supplementary figure 4: Blood flow cytometry staining of T lymphoma cells and residual normal T lymphocytes. Cell surface staining was performed on fresh blood cells during clinical T-cell lymphoma relapse (before gemcitabine treatment), with an appropriate antibody cocktail to focus on T lymphocytes: CD3-BV421 or -APC-AF750 (UCHT1), TCR $\alpha\beta$ -PE (IP26A), TCR $\gamma\delta$ -FITC (Immu510), CAR-Biotin (FMC63), Biotin Antibody-PE (REA746), CD4-PE-Cy7 (SFC112T4D11), CD8-APC-AF750 (B9.11), CD30-PE (HRS4), CD2-FITC (S5.2), CD5-PC5.5 (BL1a), CD7-PE (M-T701). Data were acquired on an 8-colour FACSCanto II flow cytometer and analysed using FACSDiva software (BD Biosciences), except for CAR* staining (data were acquired on a DxFLEX and analysed using CytExpert v2.0.2.18 software, Beckman Coulter Life Sciences).

T lymphoma cells, represented in black, can be readily identified based on their distinctive phenotypic profile: they are positive for CD3, with a low intensity, TCR $\gamma\delta$, and CD30. T lymphoma cells lack the other pan-T markers (CD4/CD8/CD2/CD5/CD7 negative), contrary to normal residual T lymphocytes represented in green. Importantly, T lymphoma cells do not express CAR.